Progress In Electromagnetics Research M, Vol. 112, 139–149, 2022

Propagation Measurements and Modelling of Natural Tropical Caves

Qi Ping Soo[1], Soo Yong Lim[1, *], Irfan F. M. Rafie[1], David Wee Gin Lim[1], Kian Meng Yap[2], and Sian Lun Lau[2]

Abstract—Caves are a vital environment with an understudied propagation characteristic to date. In this paper, we investigate the propagation environments of three tourist caves in Malaysia at 900 MHz, 2.4 and 5.8 GHz. Path loss exponents are derived from measurement data for line-of-sight (LoS) and non-line-of-sight (NLoS) sections for vertical-vertical (VV) and horizontal-horizontal (HH) polarizations. Channel fading effects are subsequently analyzed. Beyond the conventional method of computing the path loss exponent values, machine learning is also incorporated into the processing of data for yielding optimum results. The findings of this work lay a good foundation towards a greater understanding of the propagation scenarios in natural tourist caves, and they help towards establishing reliable wireless communications inside such environments.

1. INTRODUCTION

This paper reports the measurement results collected from natural caves in a tropical country Malaysia. In a previous study, it was suggested that a deterministic approach worked best for cave environments [1], which motivated us to study the propagation environments of tropical natural caves by conducting field measurement in three selected caves, namely, Jeff's Cellar Cave (JC), Kek Lok Tong Cave (KLT), and Nam Thean Tong Cave (NTT). Measurements were conducted at three frequencies, 900 MHz, 2.4 GHz and 5.8 GHz, which were similar to the frequencies used in [1], i.e., 868 MHz, 2.4 GHz and 5 GHz. The key difference is that a wireless sensor network was used in [1] as the authors found it to have great potential because communication systems for speleology (the study or exploration of caves) and potholing were wired, including systems used by emergency and rescue teams like firefighters. In the present study, we are keen to study how signals propagate inside the tropical natural caves environment, hence, wireless communication instead of wired communication becomes the subject of interest. It means that in this study, we are dealing with the random behavior of signals obstructed by stalagmites and stalactites inside caves, as contrast to a more stationary and predictable wired channel. Also, our study differs from the more predictable features of man-made caves in which smoother walls are present [2].

In a different precedent study, the author found that the fields propagating inside caves were a complex-valued Gaussian random process by the central limit theorem and showed that the probability density function for random field amplitude propagating inside a cave was Ricean [3]. Findings such as this imply that there exists a dominant signal component such as a line-of-sight (LoS) propagation path. This prompts us to investigate an immediate question arising from the previous findings. What happens when the LoS signal is lost? How well will the signal still propagate in the absence of a dominant ray path? To answer these questions, we have set up two main sections in each of the three caves, namely, LoS, and non-line-of-sight (NLoS) sections.

The underlying concern is that the propagation environment of natural caves should be carefully studied. This is especially important for tourist caves that see frequent people movement inside.

Received 14 June 2022, Accepted 26 July 2022, Scheduled 4 August 2022
* Corresponding author: Soo Yong Lim (Grace.Lim@nottingham.edu.my).
[1] Department of Electrical and Electronic Engineering, University of Nottingham Malaysia Campus, Jalan Broga, Semenyih, Selangor 43500, Malaysia. [2] School of Science and Technology, Sunway University, Jalan Universiti, Bandar Sunway, Selangor 47500, Malaysia.

Ensuring that wireless communications are available inside these caves can go a long way in the search and rescue operation when the needs arise.

Fundamentally, establishing reliable communications inside natural caves is a crucial aspect that safeguards not only the operation of speleology, but also the activity of spelunking (the exploration of caves as a hobby). Unlike propagation in tunnels and other enclosed spaces such as underground mines, which have been more thoroughly explored since the seventies, the propagation of radio waves in caves is still largely an unknown to this day, especially for tropical caves in South East Asia.

The reason behind the scarcely studied radio wave propagation in natural caves is evident. Due to the irregular wall faces of caves and the varying dielectric parameters of the cave formations, it is difficult to provide an accurate description of the criteria affecting radio wave propagation in caves. In most cases, as we walk along the walkway through the caves we will see that a variety of stalactites, stalagmites, and other cave formations evolve and develop over time. The variable conditions of caves particularly from the geometric configuration perspective make any theoretical and numerical studies of radio wave propagation in caves difficult, leaving only the empirical approach as the most feasible way for conducting propagation prediction in caves [4–6]. Nevertheless, this trend has seen a slight change of late as other methods have also been used to study the cave environment. For instance, 3D laser scanning was performed in a cave environment in Western Belize [7]. In [7], the use of 3D technologies was deemed helpful to comprehend how the space in caves was used in the past for rituals and ceremonies. In yet another more recent example, LiDAR and ray-tracing technique have been utilized to study the propagation environment of caves [8].

2. THE SELECTED CAVES IN MALAYSIA

Malaysia is home to many caves, and some of them are the biggest and longest in the world. The caves in Gunung Mulu National Park, Sarawak, for instance, have been inscribed as a World Heritage site since year 2001, and the caves have consistently attracted tourists as well as adventurous cave explorers from near and far every year. While some caves in Malaysia are used as a recognized religious temple (e.g., the famous Batu Caves near Kuala Lumpur), others are preserved archaeological sites, and still others are gorgeous with stalagmites, stalactites, and even some underground rivers flowing through the caves.

In Malaysia, caves are mostly formed out of limestone and dolomite, due to the movement of groundwater into a contemporary drainage basis. Kek Lok Tong Cave is situated in a huge cave in the limestone outcrops behind Gunung Rapat, Ipoh. The name Kek Lok Tong is translated as Cave of Ultimate Bliss or Great Happiness, and many locals regard this cave as one of Ipoh's most splendid cave temples. This cave temple sits on a 12-acre site and was used as early as 1920 as a place of worship. In 1960, the cave became part of an iron mining site [9]. When mining ceased, this cave was dedicated again to religious purposes and opened to visitors in the 1970s. Figure 1 depicts the measurement site at Jeff Cellar [6], while Figure 2 shows the measurement site at Kek Lok Tong, where spacious cavern with large openings can be seen, and the top view of this cave is displayed.

On the other hand, Nam Thean Tong Cave is a temple cave located in Ipoh. Nam Thean Tong is translated as Cave of the Southern Sky, with "southern sky" referring to heaven. This is one of Ipoh's oldest cave temples established in the year 1867 by a Chinese priest called Kuong San Teik. Figure 3 shows a glimpse of the facade inside this cave and also illustrates its geometry, in which LoS and NLoS sections can be clearly seen, consistent with the measurement sites of the two other caves.

A common feature about these three caves is that they are all natural limestone caves, and they are all tourist caves. Because of that, all three caves have been "renovated" in a way to make it suitable for tourists. For instance, all three caves' floors have been modified in a way to make walking easier inside the caves. Their floors are either covered with wooden panel or cement floors. Hence, in all three caves, the ground is a smooth surface. Nonetheless, the surrounding cave surfaces including the top and sides are kept original with flowstones, stalactites, and stalagmites protruding, which makes it ideal for us to investigate how wave propagates through the rough surfaces and stalactites inside such environment.

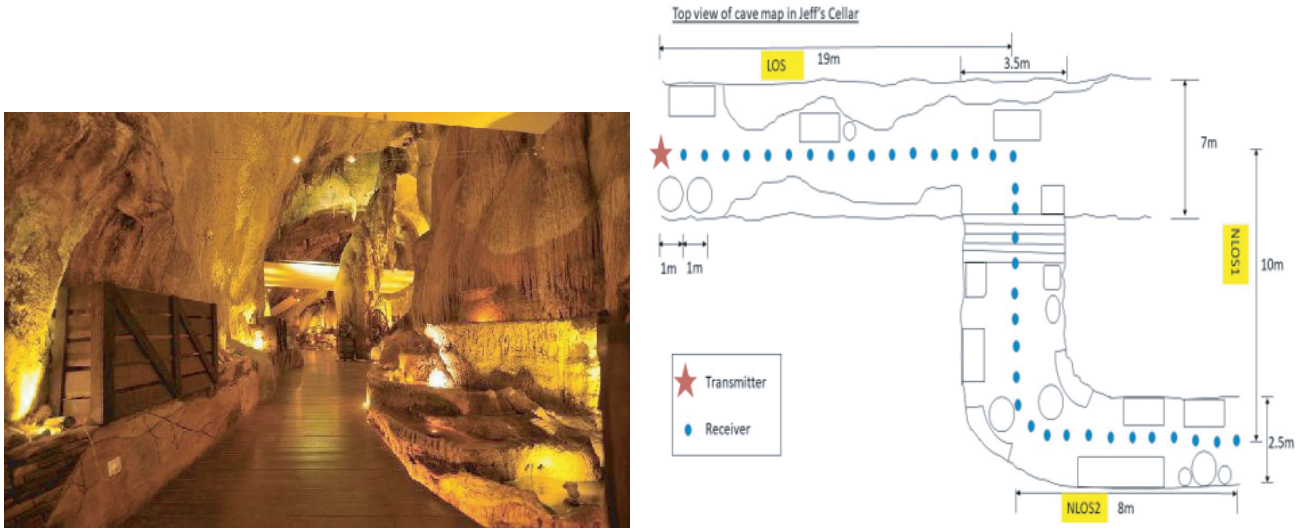

(a) (b)

Figure 1. The (a) measurement site and (b) top view of Jeff's Cellar (not to scale) [6].

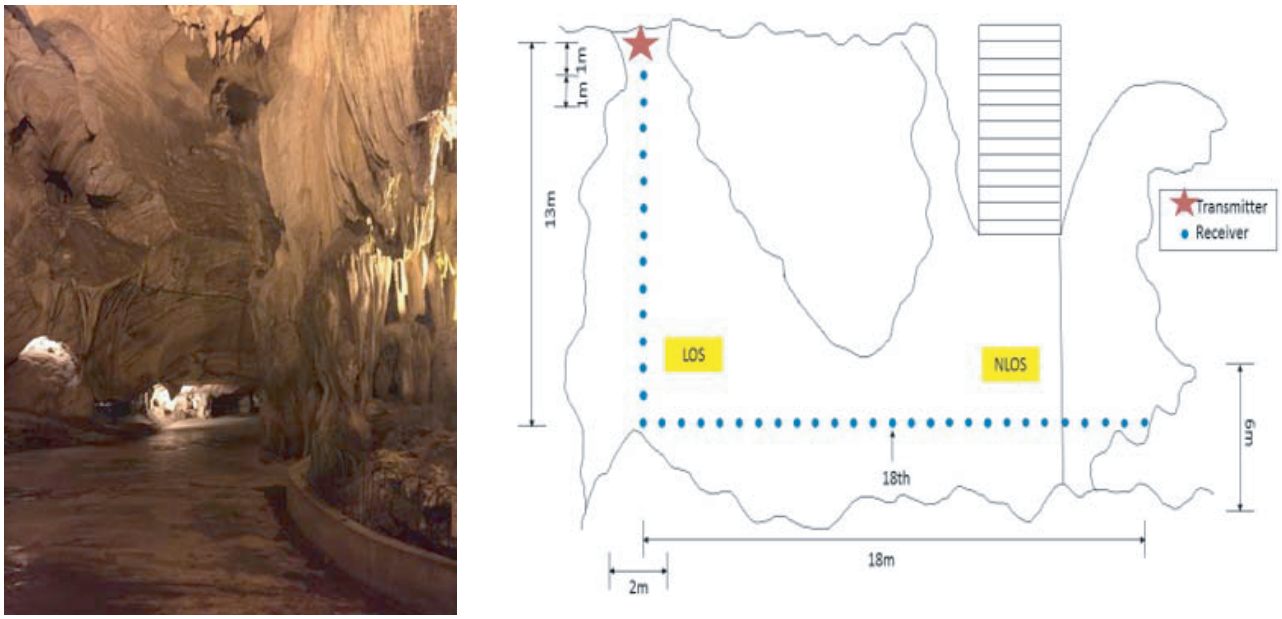

(a) (b)

Figure 2. The (a) measurement site and (b) top view at Kek Lok Tong Cave (not to scale).

3. DATA ACQUISITION UNIT

We have carried out field measurement campaign at three distinct frequencies, namely, 900 MHz, 2.4 and 5.8 GHz. These are common frequency bands as we deem them essential and appropriate for an understudied propagation environment like tropical natural caves. To elaborate further, 900 MHz is known for its capability of long-range communication in elliptical and curved passage and may be highly relevant to wireless communication in caves. As for 2.4 GHz, it has been used extensively in Bluetooth wireless communication while 5.8 GHz is commonly employed for broad application to digital communication comprising IEEE 802.11x Wi-Fi. These two frequency bands may also be highly relevant

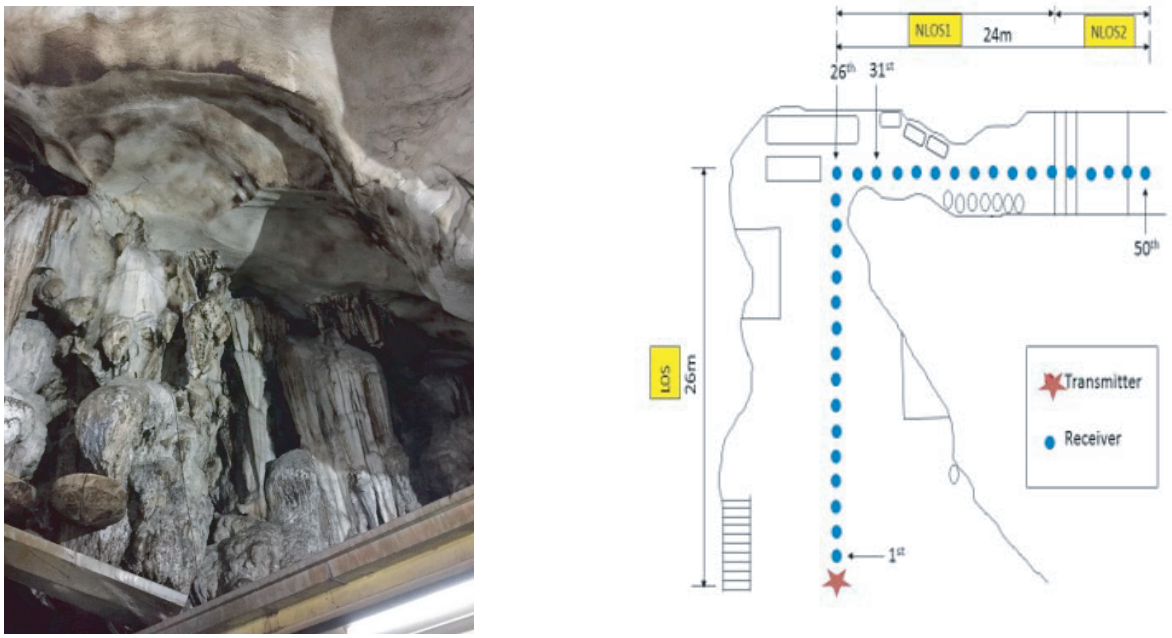

(a) (b)

Figure 3. (a) A glimpse of the façade inside Nam Thean Tong Cave and (b) Top view of Nam Thean Tong Cave (not to scale).

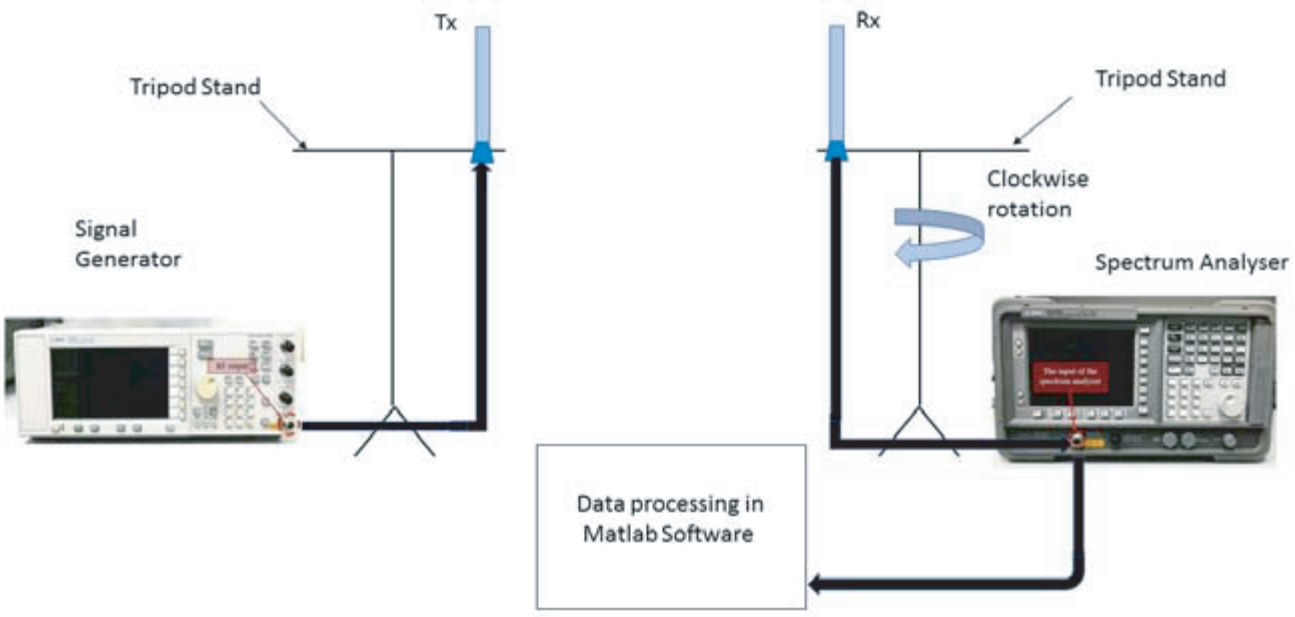

Figure 4. Measurement system setup.

for cave environments. Figure 4 shows the block diagram of the assembled Data Acquisition Unit while Table 1 lists the specific items.

From Figure 4, it can be seen that the transmitter (Tx) antenna was connected to a signal generator, and then placed at a static location to transmit signal at the three frequencies, see the red stars in Figures 1 to 3 for all three caves. As for the receiver (Rx) antenna, it was mounted on a 33 cm long wooden rod attached to a tripod, and afterwards rotated 360° at every Rx location. In each

Table 1. The equipment list for the measurement system.

Equipment	Specifications	Model
900 MHz Antenna	6 dBi wireless omnidirectional antenna	L-Com HGV-906U
2.4 GHz Antenna	8 dBi omnidirectional wireless-LAN antenna	HyperLink Technologies HGV-2409U
5.8 GHz Antenna	8 dBi ISM/UNII band omnidirectional wireless-LAN antenna	HyperLink Technologies HG5808U
Transmitter (Tx)	Analog Signal Generator, 250 kHz to 6 GHz	Agilent E4428C
Receiver (Rx)	Spectrum Analyzer, 9 kHz to 6.7 GHz	Agilent E4404B
Cables	FLEX CA NM/NM 15FT RoHS	CBL− 15FT− NMNM+

location, 400 received signals were recorded and averaged to yield a single mean value, hence eliminating the small scale fading effects. The received signal strength was displayed on a spectrum analyzer, stored, and subsequently transferred onto a computer for post-processing on MATLAB. Omnidirectional antennas were oriented for co-polarizations such as vertical-vertical (VV) and horizontal-horizontal (HH) polarization throughout the measurement campaigns. The height of the Tx and Rx antennas, along with their polarization at each frequency for each cave, are recorded and presented in Table 2.

Table 2. The antenna heights of Tx and Rx.

Frequency and polarization		Jeff Cellar Cave (METERS)		Kek Lok Tong Cave (Meters)		Nam Thean Tong Cave (Meters)	
		Tx	Rx	Tx	Rx	Tx	Rx
900 MHz	VV	1.50	1.50	1.65	1.65	1.7	1.7
	HH	0.98	0.96	1.15	1.15	1.19	1.19
2.4 GHz	VV	1.40	1.40	1.58	1.58	1.62	1.62
	HH	0.90	0.90	1.15	1.15	1.24	1.24
5.8 GHz	VV	1.25	1.27	1.38	1.38	1.45	1.45
	HH	0.90	0.90	1.15	1.15	1.17	1.17

4. MEASUREMENT RESULTS OF CAVES

The first cave JC consists of a cavern with a LoS region of 1 m to 18 m and an NLoS region of 22 m to 37 m. The turning point occurs at a region between 19 m and 21 m. The second cave KLT consists of a passage with a LoS region of 1 m to 17 m and an NLoS region of 21 m to 31 m. The turning point occurs at a region between 18 m and 20 m. The third cave NTT consists of a cavern passage with a LoS region of 1 m to 26 m and an NLoS1 region occurring at between 32 m and 40 m and NLoS2 region occurring at between 43 m and 50 m. The first turning point takes place at between 27 m and 31 m, while the second turning point takes place at between 41 m and 42 m. In Figure 5, the co-polarization effects of NTT Cave are presented at the above-mentioned frequencies.

From the co-polarization results we collected from all three caves, we observe a consistent trend of VV-polarization being stronger than HH-polarization at every frequency, for both LoS and NLoS sections. It is also evident to note that 900 MHz signal propagates more strongly than 2.4 GHz. Likewise, 2.4 GHz signal propagates more strongly than 5.8 GHz. This observation holds for the results of all three caves. In addition, we note that HH polarization tends to fluctuate more than VV polarization, which implies that HH polarization is more sensitive to the elliptical passage of the cave and to the stalactites. To better consolidate our findings, Table 3 is presented to show the path loss exponent n values as

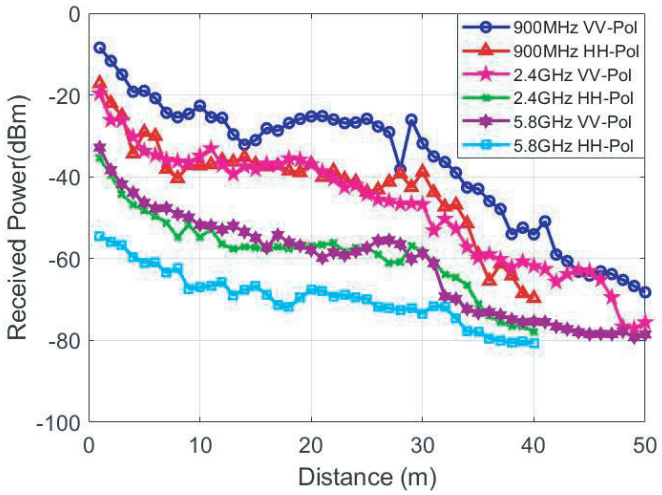

Figure 5. The measurement results collected from the third cave Nam Thean Tong.

Table 3. The path loss exponent and standard deviation values.

Freq	Cave/Pol	Path Loss Exponent, n		Standard deviation, σ (dB)	
		LoS	NLoS	LoS	NLoS
900 MHz	1)JC/VV	1.65	2.45	0.98	2.25
	2) JC/HH	1.85	2.54	3.79	1.90
	3) KLT/VV	2.14	0.93	2.55	2.07
	4) KLT/HH	1.46	1.92	3.14	2.62
	5) NTT/VV	1.37	3.17	2.62	5.50
	6) NTT/HH	1.58	3.04	2.58	5.31
	Average	**1.68**	**2.34**	**2.65**	**3.28**
2.4 GHz	1) JC/VV	1.77	1.75	1.57	1.58
	2) JC/HH	1.31	1.41	2.89	0.75
	3) KLT/VV	1.80	0.78	1.45	2.01
	4) KLT/HH	1.46	1.52	2.57	1.25
	5) NTT/VV	1.45	2.24	2.18	3.86
	6) NTT/HH	1.62	2.01	1.55	3.73
	Average	**1.57**	**1.62**	**2.04**	**2.20**
5.8 GHz	1) JC/VV	1.55	0.73	1.85	1.25
	2) JC/HH	1.35	0.87	2.24	0.60
	3) KLT/VV	1.71	0.80	0.95	1.13
	4) KLT/HH	1.74	0.60	2.14	1.05
	5) NTT/VV	1.85	1.89	1.16	1.73
	6) NTT/HH	1.31	0.95	1.54	2.04
	Average	**1.59**	**0.97**	**1.65**	**1.30**

well as the standard deviation values computed for both LoS and NLoS sections for all three caves at the two polarizations. Because the average n values are computed from three individual caves of like characteristics, they are more convincing and can be used for propagation prediction of other similar caves elsewhere.

In the computation of n values, we have firstly assumed all n values to be between 1 and 15 with an interval of 0.01. When the best n-values are determined, the standard deviation σ_m (dB) between the measured path loss and the predicted path loss by (1) is at the most minimum.

$$P(d)\,[\text{dB}] = \bar{P}(d_0)\,[\text{dB}] + 10n\log_{10}\left(\frac{d}{d_0}\right) + X_\sigma\,[\text{dB}] \tag{1}$$

In (1), $P(d)$ is the path loss/gain in dB, $\bar{P}(d_0)$ the reference path loss at a distance d_0 from Tx, d the distance to the source, and X_σ the log-normal distribution. In essence, path loss is an indication of power loss in the channel, and in this case, the caves environment.

When the n values and standard deviation values in Table 3 are calculated, one transition point between the LoS and NLoS sections has been excluded. This explains why the earlier reported NLoS path loss exponent values were higher for Jeff Cellar because in that preceding work, no transition points were dropped in the calculation [6]. We reckon in this study that dropping the transition points is a more reasonable approach as that can better portray the real scenario, hence improving the accuracy of the results, which is reflected by a more realistic n value and a lower standard deviation value. As can be seen from Table 3, there exists a wave-guiding effect in all sections of the caves, and this is exemplified by the one-something n-values. Apart from the obvious drop of signal when turning from LoS to NLoS section, when turning from NLoS1 to NLoS 2 for NTT Cave, there is no more drastic drop of signal, and yet the wave-guiding effects remain. This observation is consistent with what was reported in a block cave gold mine at 915 MHz, that in the LoS section a low n-value of 1.25 was reported in year 2021 [10]. In a similar manner, in the NLoS section, good propagation was noted as well. In this block cave gold mine work, the author concluded that the propagation behavior might be the consequence of waveguide behavior of the steel lined tunnel. His conclusion testified to what is summarized in Table 3, which has good propagation in both LoS and NLoS sections, and a wave-guiding effect in caves. From this we can assert that if we want signal to propagate sufficiently strong into the deeper part of the cave, a stronger transmitting signal should be supplied at the entrance of the cave, even with the use of a high power amplifier. This may be particularly useful for search and rescue operation when the needs arise, when entering the deeper part of the cave is required, just like the case of the Thai football team who was lost and found in 2018 [11].

5. CHANNEL FADING EFFECTS INSIDE CAVES

In this section, we present our findings on channel fading effects inside caves. This is done by investigating the precise fading characteristics through computing the Cumulative Distribution Function (CDF) of fading distribution of the received signals. The comparison of Rician, Rayleigh, and Lognormal fading distributions is presented in the subsequent figures, Figures 6 and 7. At first, Rician fading happens when there is a dominant ray propagation from line-of-sight (LoS), as governed by Equation (2).

$$f_{rician}(r) = \frac{r}{\sigma^2}e^{\left(\frac{-r^2+A^2}{2\sigma^2}\right)}I_o\left(\frac{Ar}{\sigma^2}\right) \tag{2}$$

where I_o is a modified Bessel function of the first kind and of zero order, σ^2 the average power of the received fading signal, A the peak amplitude of the dominant signal, r the received signals, and the Rician distribution is generally defined in terms of parameter $K = Ar/2_{\sigma^2}$. On the other hand, Rayleigh fading would occur when there is no line-of-sight propagation between the transmitter and receiver, as governed by Equation (3).

$$f_{rayleigh}(r) = \frac{r}{\sigma^2}e^{\left(\frac{-r^2}{2\sigma^2}\right)} \tag{3}$$

whereas for log-normal fading distribution, it is broadly utilized to characterize the NLoS propagation path loss, especially during ray penetration through walls or windows and through enormous obstacles. It is worth pointing out that the log-normal distributed random variable does in fact obey a normal or Gaussian distribution when the values are measured in decibels. It is described in terms of a probability function as listed in Equation (4) [12].

$$p(x) = \frac{1}{\sqrt{2\pi\sigma}}e^{\frac{-(x-\mu)^2}{\sigma}} \tag{4}$$

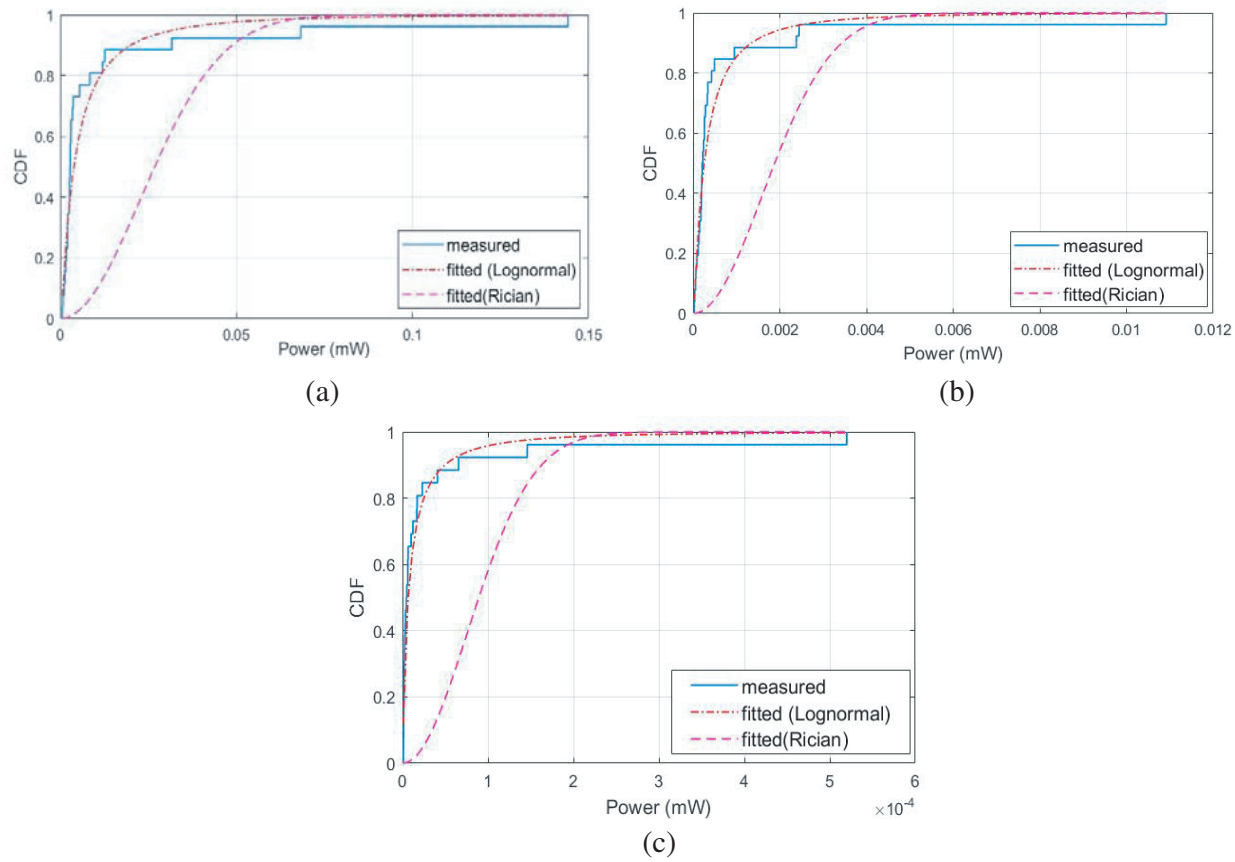

Figure 6. The measured and modeled distribution of the received signal for VV Polarization at (a) 900 MHz, (b) 2.4 GHz and (c) 5.8 GHz in LoS region.

In Figure 6, the measured path loss data were compared with Rician and Log-normal ones. We observe that Log-normal distribution is closely matched with the measured data. It shows that more penetration loss of signals is due to the stalagmites and stalactites.

In Figure 7, we compare the measured path loss data with the theoretical distribution such as Log-normal and Rayleigh ones. We find that the log-normal distribution obtains a better fit with the measured data than the other distributions.

6. MACHINE LEARNING

Artificial intelligence is fast embedded into many fields, including electromagnetics, antennas, and propagation. In this section, we further process our measurement data with machine learning techniques and present our findings. In particular, we reprocess the power drop at the transition from LoS to the NLoS section, and analyze its impact on the resulting n-values and standard deviation values using a clustering model. This model is chosen due to the sharp increase in path loss seen at the transition points which would help the model determine whether a path loss change is detected. The number of clusters chosen is 2 for LoS and NLoS areas from prior knowledge of the cave's geometry. Nevertheless, as the complexity of the cave network increases, this value may have to be chosen using a different method. The amount of power drop when transitioning from LoS to NLoS is defined as the amount of signal strength lost when transitioning from LoS A to LoS B where $N-1$ is a data point in LoS A, $N+1$ a data point in LoS B, and N the exact location of the LoS. In our test, the training is supported by several key data extracted from the cave which are the type of corner (open corner, closed corner, T-junction), the size of entrance (surface area of cross section of cave at location $N-1$), the size of exit

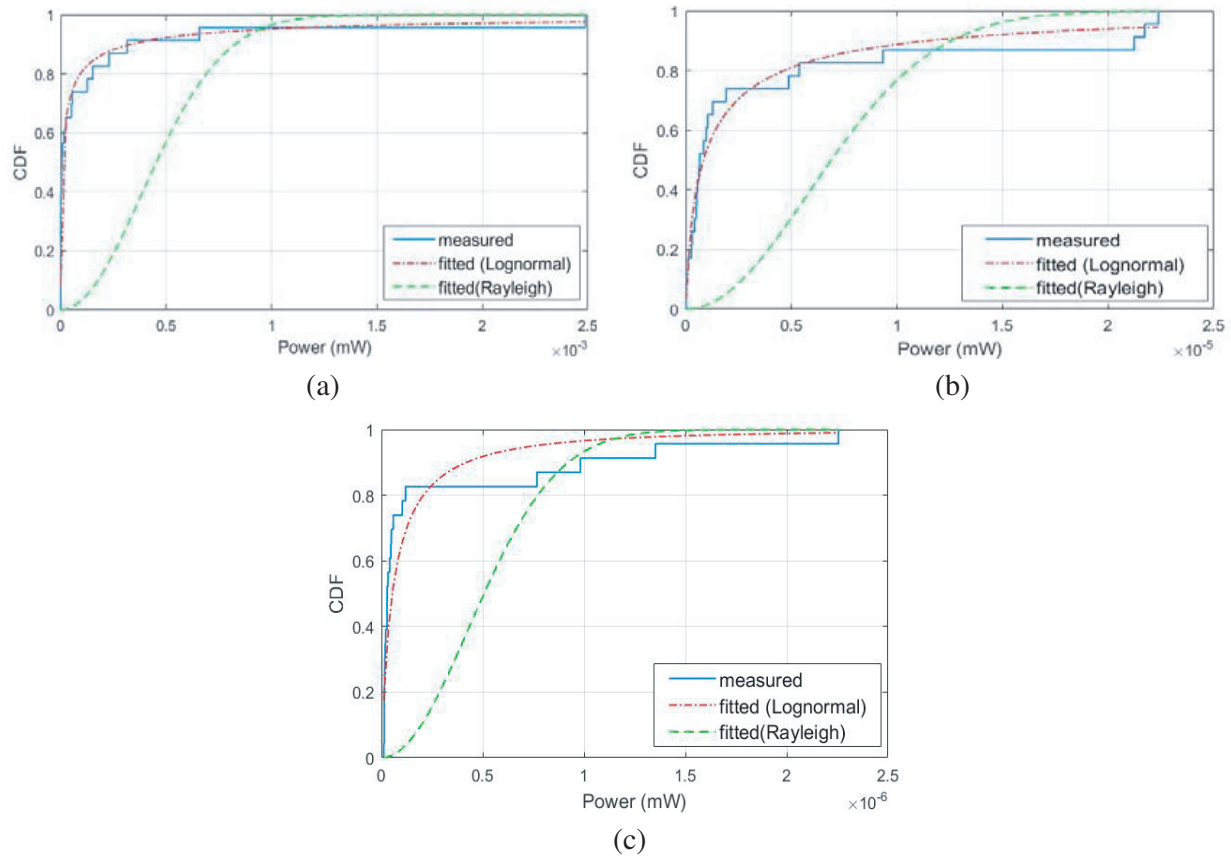

Figure 7. The measured and modeled distribution of the received signal for VV Polarization at (a) 900 MHz, (b) 2.4 GHz, (c) 5.8 GHz in NLoS region.

(surface area of cross section of cave at location $N+1$), and the angle change of LoS (measured at the point of intersection of all 3 data points). Table 4 lists the n-values as well as the standard deviation values computed for both LoS and NLoS sections with machine learning for all three caves at the two polarizations.

The difference between Table 3 and Table 4 is that the results obtained from Table 3 were determined manually, while the results in Table 4 were obtained from K-means clustering. Using K-means clustering, it is possible to cluster these data points into their own clusters, i.e., LoS. By assigning the number of clusters or change in LoS paths, K-means clustering is able to predict which cluster a data point belongs to and more importantly, the transition point between the two sections, N. However, since K-means requires the number of clusters to be preset for the algorithm to work, this must be done by assigning a higher cluster count than the number of corners a cave has and reduced using the amount of signal strength drop as a reference. Future research into this area may yield results in determining the features of a cave or change in the LoS to NLoS sections without prior data.

By using the geometric features of the caves such as the width, height, and distance as training attributes, with measured path loss as prediction value, we were able to predict path loss values in all three caves. However, due to (still) limited data, generalization at this moment is not as accurate for all natural caves. This leaves room for future research into this area, for more measurements to be conducted from more researchers worldwide collectively in a great variety of caves in the world.

Table 4. The k-means (path loss exponent and standard deviation values).

Freq.	Cave/Pol	Path Loss Exponent, n			Standard deviation, σ (dB)		
		LoS	NLoS1	NLoS2	LoS	NLoS1	NLoS2
900 MHz	1) JC/VV	1.82	0.72	1.99	0.60	3.04	2.53
	2) JC/HH	1.12	1.53	1.62	2.79	4.05	1.89
	3) KLT/VV	1.91	1.23	-	0.66	2.23	-
	4) KLT/HH	1.49	1.92		2.98	2.51	-
	5) NTT/VV	1.72	0.29	2.33	1.29	4.11	2.77
	6) NTT/HH	1.67	0.60	1.98	2.88	2.19	2.02
	Average	**1.62**	**1.05**	**1.98**	**1.87**	**3.02**	**2.30**
2.4 GHz	1) JC/VV	1.81	0.74	1.17	1.03	3.62	1.10
	2) JC/HH	1.10	0.41	1.06	2.49	4.84	0.57
	3) KLT/VV	1.80	0.91	-	1.41	1.79	-
	4) KLT/HH	1.30	1.63	-	2.27	2.50	-
	5) NTT/VV	1.28	1.20	1.38	1.98	1.74	3.89
	6) NTT/HH	1.88	0.20	1.70	1.15	1.27	1.53
	Average	**1.53**	**0.85**	**1.33**	**1.72**	**2.63**	**1.77**
5.8 GHz	1) JC/VV	1.15	0.39	0.73	1.54	1.49	1.21
	2) JC/HH	1.35	0.77	0.01	2.18	1.17	0.00
	3) KLT/VV	1.71	1.15	-	0.92	1.05	-
	4) KLT/HH	1.47	0.74	-	1.72	1.42	-
	5) NTT/VV	1.80	0.30	0.84	0.51	1.59	0.60
	6) NTT/HH	1.30	0.22	0.95	1.42	1.48	1.96
	Average	**1.46**	**0.60**	**0.63**	**1.38**	**1.37**	**0.94**

7. CONCLUSION

Caves are a unique environment that has played a vital role in the evolvement of mankind. Just like human beings, every cave is different and has its own distinct feature. It makes collecting as many measurement results from as many caves important, for they collectively help towards making reliable wireless communications inside caves palpable. It is for this purpose that we have collected a series of measurement results inside three natural caves frequented by tourists in Malaysia, a tropical country with Monsoon seasons. Path loss exponent values are computed for the co-polarizations — VV and HH alike for all three caves at the three frequencies. Subsequently, the average path loss exponent values are computed, and it is shown that there exists a wave-guiding effect inside caves, in both the LoS and NLoS sections. Channel fading effects are analyzed, and we find that the log-normal distribution obtains a better fit with the measured data than the other distributions. Lastly, we have utilized machine learning to process the measurement data for additional comparison. The findings of this work have real and practical implications, and its impact can be most visibly seen in the cave rescue operation should the needs arise.

REFERENCES

1. Laborra, T., L. Azpilicueta, P. L. Iturri, E. Aguirre, and F. Falcone, "Estimation of wireless coverage in complex cave environments for speleology applications," *Proc. USNC-URSI Radio Sci. Meeting*, 120, Memphis, TN, USA, Jul. 2014.

2. Zhou, C., T. Plass, R. Jacksha, and J. Waynert, "RF propagation in mines and tunnels," *Antennas and Propagation Magazine*, Vol. 57, 88–102, IEEE, 2015.
3. Pao, H. Y., "Probability density function for waves propagation in a straight rough wall tunnel," *Proc. IEEE Int. Symp. Antennas Propag.*, 2975–2978, Monterey, CA, USA, Jun. 2004.
4. Rak, M. and P. Pechac, "UHF propagation in caves and subterranean galleries," *IEEE Transactions on Antennas and Propagation*, Vol. 55, 1134–1138, Apr. 2007.
5. Bedford, M. D. and G. A. Kennedy, "Modeling microwave propagation in natural caves passages," *IEEE Transactions on Antennas and Propagation*, Vol. 62, No. 12. 6463–6471, 2014.
6. Soo, Q. P., S. Y. Lim, D. W. G. Lim, K. M. Yap, and S. L. Lau, "Propagation measurement of a natural cave-turned-wine-cellar," *IEEE Antennas Wirel. Propag. Lett.*, Vol. 17, No. 5, 743–746, 2018.
7. Lindgren, S. and F. Galeazzi, "3D laser scanning in cave environment: The case of las cuevas, belize acquisition of the cave system and excavation area," *Proc. 2013 Digital Heritage International Congress (Digital Heritage)*, Marseille, France, Oct. 28–Nov. 1, 2013.
8. Bedford, M. D., A. Hrovat, G. Kennedy, T. Javornik, and P. Foster, "Modeling microwave propagation in natural caves using LiDAR and ray tracing," *IEEE Transactions on Antennas and Propagation*, Vol. 68, No. 5, 3878–3888, 2020.
9. "Tin Mine Cavern Gua Tempurung," accessed on Jun. 3, 2022, [Online], Available: Ipoh City Attration — Kek Lok Tong (ipoh-city.com).
10. Branch, P., "Propagation measurements and models of 915 MHz LoRa radio in a block cave gold mine," *Proc. 2021 Int. Conf. on Information Networking*, 333–338, Jeju Island, Korea (South), Jan. 2021.
11. "Tham Luang Cave Rescue," accessed on Jun. 3, 2022, [Online], Available: Tham Luang cave rescue — Wikipedia.
12. Rappaport, T. S., *Wireless Communications: Principles and Practice*, 2nd Edition, Prentice Hall, Upper Saddle River, NJ, USA, 2002.